J Mater Sci: Mater Electron (2017) 28:625–632
DOI 10.1007/s10854-016-5567-1

Investigation of site selectivity of lanthanum in $SrBi_4Ti_4O_{15}$ ceramic by structural, dielectric, ferroelectric and conduction behavior

P. Nayak[1] · T. Badapanda[2] · S. Panigrahi[1]

Received: 15 July 2016 / Accepted: 16 August 2016 / Published online: 2 September 2016

Abstract This manuscript reports the structural and electrical properties of Lanthanum substituted strontium bismuth titanate with general formula $SrBi_{4-x}La_xTi_4O_{15}$ (where $0 \leq x \leq 0.25$), prepared by solid-state reaction route. X-ray diffraction study shows a single phase orthorhombic structure in all the compositions. It was also observed that the lattice parameter increases up to $x = 0.15$ and then decreases with further La content. The Raman spectra shows the distribution of lanthanum into the perovskite layers and $(Bi_2O_2)^{2+}$ layers of $SrBi_4Ti_4O_{15}$ ceramic. The temperature dependent dielectric study reveals that the transition temperature and maximum dielectric constant decreases with La content. The broadening of the phase transition was observed with La substitution due to the decrease in octahedral distortion. Impedance analysis confirms the presence of two semicircular arcs in doped samples, suggesting the existence of grain and grain-boundary conduction. The P-E loop study shows that both the remnant polarization (P_r) and the coercive field increases with the increasing La content up to $x = 0.15$ and thereafter decreases to lower values with further La content. Similar kind of trend is also observed in DC conductivity.

✉ P. Nayak
priyambada.pce@gmail.com

[1] Department of Physics and Astronomy, National Institute of Technology, Rourkela, Odisha 769008, India

[2] Department of Physics, C.V. Raman College of Engineering, Bhubaneswar, Odisha 752054, India

1 Introduction

Strontium Bismuth Titanate [$SrBi_4Ti_4O_{15}$ (SBT)] is a well-known member of the bismuth oxide layer structure ferroelectric (BLSF) material and has the potential for application in sensors, actuators, high-temperature piezoelectric applications, and memory storage devices (ferroelectric NvRAM) [1, 2]. The SBT ceramic has high Curie temperature ($T_c = 530$ °C) but the piezoelectric properties are comparatively lesser than that of a lead based system [3]. It has orthorhombic symmetry with space group $A2_1am$ at room temperature and transforms to tetragonal space group *I4/mmm* above the transition temperature [4]. The major drawback with the SBT material is the volatilization of bismuth during the sintering process at high temperature in solid state reaction method. The bismuth volatilization leads to the formation of oxygen vacancy in order to maintain the charge neutrality. Oxygen vacancy might be preferably present in the vicinity of the Bi ions which could dramatically decreases the properties [5]. This oxygen vacancy plays an important role in determining the fatigue property of a ferroelectric material. Chu et al. [6] reported that fatigue is caused by the diffusion of oxygen vacancies to the domain walls and subsequently pinning the domain walls. Furthermore, previous studies have found that the oxygen vacancy is the dominant point defect in oxide feroelectric materials [7]. It has also been regarded as the cause of many detrimental effects such as pinning domain walls, screening the electric field near the space charge region, impeding the displacement of the Ti^{4+} ion, trapping charge carriers, and enhancing leakage current [8–10]. This oxygen vacancy is also responsible for increase in conductivity of the material. For industrial application as memory, it is necessary to obtain materials with low dielectric loss, low conductivity and high fatigue

properties. In order to minimize the drawback associated with oxygen vacancy, as well as to tailor the ferroelectric properties of BLSFs, many studies have been reported on A and/or B-site substitutions in SBT. Recently, efforts have been made to enhance the properties of layer perovskites by substitution the Bi^{3+} by alternative cations. Moreover, substitution of stable trivalent lanthanide ions for volatile bismuth ions was effective for suppressing oxygen vacancy concentration and increasing the chemical stability of the Perovskite layers which strongly affect the electrical properties [11, 12]. On the other hand, some researchers found that among the lanthanoidal dopants, La^{3+} (Lanthanum) is frequently added to other bismuth-based layer perovskite ceramics in order to lower its tanδ value with decrease in conductivity, improvements in ferroelectric properties, and improved fatigue resistance [13–15]. Chakrabarti et al. [16] observe that La^{3+} substitution for Bi^{3+} at the A-site in $BaBi_{4-x}La_xTi_4O_{15}$ ceramic results in a well defined relaxor behavior with a reduction in DC conductivity. Khokhar et al. [17] reported the enhancement of ferroelectric properties of La doped BBT ceramic up to 20 % of La doping. There are a few reports in the literature on La substituted $SrBi_4Ti_4O_{15}$ ceramics. It has been reported by Zhu et al. [18] that, the substitution with La^{3+} in the bulk SBT system produces a structural distortion. Chen et al. [19] reported apparently much higher level of Lanthanum ion substitution in SBT materials and determined the lattice distortion and internal stress. In these earlier studies, the structural properties of La modified $SrBi_4Ti_4O_{15}$ with a wide variation are described without any supporting evidence from dielectric and electrical study. Therefore, it motivates us to further investigate the dielectric, ferroelectric, impedance and conductivity behavior of La^{3+} modified SBT ceramics and to correlate the observed changes with the induced structural effect.

2 Experimental

The La doped SBT ceramic with chemical composition $SrBi_{4-x}La_xTi_4O_{15}$ (x = 0.00, 0.05, 0.1, 0.15, 0.2 and 0.25) was prepared by solid state reaction technique using the high purity (≥99. 9 %) ingredients $SrCO_3$, Bi_2O_3, TiO_2 and La_2O_3. The powder was mixed in stoichiometric proportion thoroughly in an acetone medium using a laboratory ball milling machine and then calcined at temperature of 900 °C for 3 h. The calcined powder was ground and then pressed into the disc at a pressure of 5×10^6 N/m^2 using a hydraulic press with PVA as a binder. The discs were sintered at a temperature of 1050 °C for 2 h in a programmable furnace with 5 °C min^{-1} heating rate. The phase confirmation of the ceramic was analyzed by X-ray diffractometer (Rigaku Ultima IV) with monochromatic Cu K_α radiation (λ = 1.54178 Å) over a 2θ range of 20° to 80° at 3°/min. The Raman scattering measurements were performed in the backscattering geometry using a Jobin–Yvon T64000 triple monochromatic equipped with large coupled detector. For electrical measurements, high purity silver electrode was applied on the opposite disc faces and were dried at 250 °C for 30 min to remove moisture. The dielectric and impedance measurements were carried out in the frequency range 100 Hz to 1 MHz using Wayner Kerr impedance analyzer. The Polarizations versus electric field (P-E) measurements were carried out by using precision premier II, a standard ferroelectric testing machine (Radiant Technology).

3 Result and discussion

3.1 X-ray diffraction study (XRD)

Figure 1 shows the X-ray diffraction pattern of $SrBi_{4-x}La_xTi_4O_{15}$ ceramics recorded at room temperature for

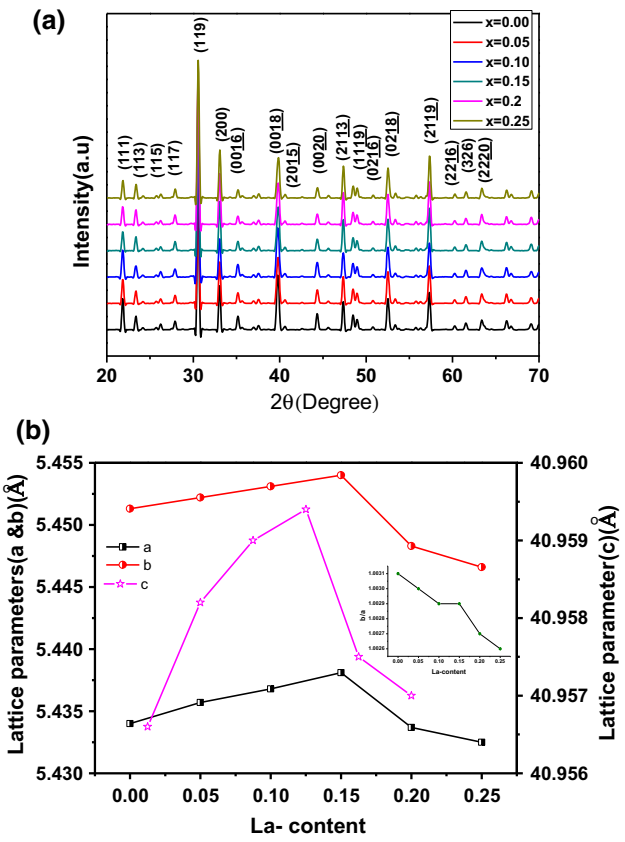

Fig. 1 **a** XRD patterns for $SrBi_{4-x}La_xTi_4O_{15}$ with composition x = 0.00, 005, 0.1, 0.15, 0.2, 0.25 at RT. **b** Variation of lattice constants with La-content

various La doping concentrations (x = 0.0, 0.05, 0.10, 0.15, 0.20 and 0.25). The XRD patterns of all composition shows a single orthorhombic phase with $A2_1am$ space group without any impurities or unwanted peak. This demonstrates that lanthanum substitution does not affect the structure and all the composition possesses a bismuth layered structure with four layers (m = 4), as reported earlier [20]. The lattice parameters were determined by the chekcell software and plotted with various La-content as shown in Fig. 1b. A marginal increase in the lattice parameter was noted for La-content up to x = 0.15 and then after it decreases with further increase in La content. The increase in the lattice parameter up to x = 0.15 may be due to the occupancy of La in the pseudo-perovskite layer [21, 22]. For higher La content (x ≥ 0.20), a slight decrease in the lattice parameters is attributed to the occupancy of La^{3+} in $(Bi_2O_2)^{2+}$ layer, over and above the occupancy in the perovskite layer [18]. The opposite changes in the lattice parameters before and after a critical La content x = 0.15, interestingly coincide with immediate changes in the electrical properties and are discussed later in the paper. Similar type of result was also reported on rare earth substitution in other layer perovskite [18, 23, 24].

3.2 Raman spectroscopy

The Raman spectrum of La-doped SBT ceramic is shown in Fig. 2a. According to structural chemistry, SBT with orthorhombic structure have two different types of vibration modes. One is the internal mode of TiO_6 octahedra and another one is the lattice transition modes related to the motion of the cations in the pseudo-perovskite slabs and Bi_2O_2 layer [25]. Some sharp phonon modes at ~155, 272, 559, 869 cm^{-1} along with some weak features were observed in Fig. 2a. All the Raman modes correspond to the characteristic modes of SBT as reported earlier [26, 27]. The low frequency modes are correlated with the motion of the heavier Bi^{3+} ions, which is assigned to the vibrations of "rigid layers" generally observed in layered structures $ABi_4Ti_4O_{15}$ (where A = Ba, Ca, Pb and Sr) [28]. The modes at 155 cm^{-1} originate from the motion of A-site ions in the pseudo-perovskite slabs, and the modes above 200 cm^{-1} having A_{1g} character correspond to the TiO_6 octahedra. The intense mode at ~272 cm^{-1} corresponds to the "rocking mode" due to the torsional bending of the TiO_6 octahedra. The mode at ~559 cm^{-1} is assigned to the opposing excursions of the external apical oxygen atoms of the octahedra and the mode at 869 cm^{-1} represents the symmetric stretching of the TiO_6 octahedra [29].

For a comparative observation of the deviations in the different modes occurring due to La substitution, the fine shifts in the Raman frequency due to compositional changes are shown in Fig. 2b. It was observed that the mode at 155 cm^{-1} shows a minimal shift up to x = 0.15 indicating pronounced hardening, and begins to shift to a higher frequency beyond x > 0.15. The asymmetric deviation in the mode clearly indicates the site selectivity of the La^{3+} ions below and above x = 0.15. The hardening of the mode at 155 cm^{-1} till x = 0.15, is attributed to the decreasing average mass of Bi/La ions (Bi/La = 208/139) due to La-substitution at the A-site. For x > 0.15, the increased shift in the mode at 155 cm^{-1} to a higher frequency with increasing Lanthanum content implies that La^{3+} ions replace Bi^{3+} ions both in the $(Bi_2O_2)^{2+}$ layer and the perovskite layer. The mode at ~272.0 cm^{-1} which corresponds to the torsional bending of the TiO_6 octahedra, shows a continuous increase to higher frequency with increasing La content. The band at ~559.0 cm^{-1} shows interesting changes with varying La content. The mode shifts to lower frequency up to x = 0.15, and begins to shift to higher frequency for x > 0.15, when the structure of the $(Bi_2O_2)^{2+}$ layers begins to get affected by La^{3+} substitution. Zhu et al. [25] have suggested that the increase in the vibration frequency of the mode at 559.0 cm^{-1} is due to the stretching of the TiO_6 octahedra which are linked to $(Bi_2O_2)^{2+}$ layers as they tend to shrink when the $(Bi_2O_2)^{2+}$ layers are affected by La substitution. Thus, at higher La content x > 0.15 the structural disorder increases due to La^{3+} incorporation into the $(Bi_2O_2)^{2+}$ layers. Similar kind of variation was also observed at 869 cm^{-1} mode.

3.3 Dielectric study

The temperature dependent dielectric constant at 100 kHz of $SrBi_{4-x}La_xTi_4O_{15}$ ceramics is shown in Fig. 3a. It was observed that the room temperature dielectric constant increases with increase in La content up to x = 0.15 and then decreases with higher concentration (as shown in Table 1). This may be due to the increase in lattice parameter 'a' and associated relaxation in the structural distortion up to x = 0.15. For higher concentration the lattice parameter decreases, which lowers the polarization [30, 31]. It was also noticed that with increasing La content, the transition temperature (T_m) shift towards lower temperature and the maximum dielectric constant (ε'_m) values decreases. The reduction in the dielectric constant may be due to the incorporation of larger ionic radii La^{3+} ion in Bi^{3+} ion which enlarges the unit cell and lattice distortion. The decrease of T_m can be explained on the basis of tolerance factor 't' given by [32]:

$$t = \frac{R_A + R_O}{\sqrt{2}(R_B + R_O)} \quad (1)$$

where R_A, R_B and R_O are the effective ionic radii for the A-site cation, B-site cation and oxygen ion respectively.

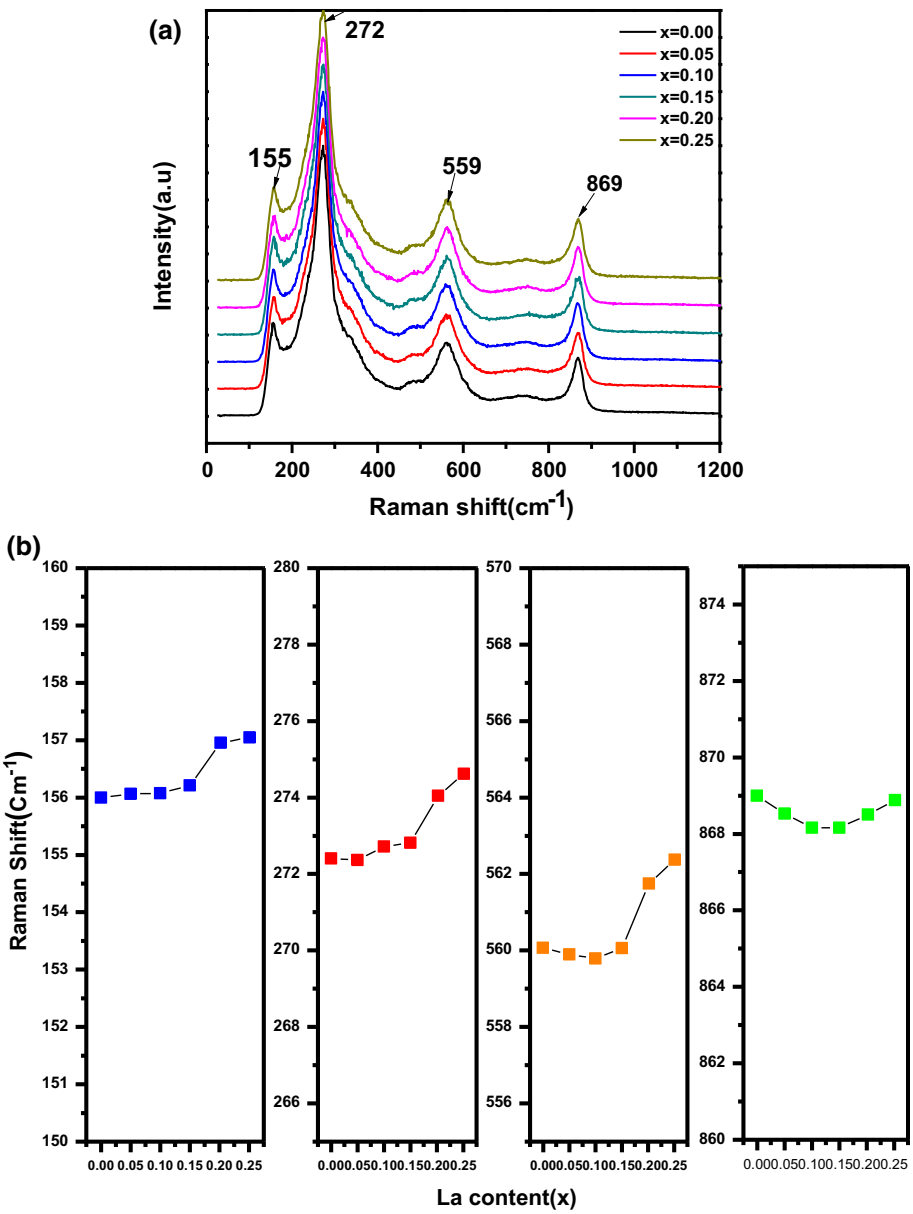

Fig. 2 **a** Raman spectra of La-doped SBT. **b** Compositional dependence of the various Raman modes for $SrBi_{4-x}La_xTi_4O_{15}$ ceramics

Since the ionic radius of La^{3+} ($\sim$0.136 nm), is larger than that of Bi^{3+} ($\sim$0.117 nm), therefore, the substitution of La^{3+} for A-site Bi^{3+}, increases the tolerance factor and hence T_m decreases [31]. Such a decrease in the phase transition temperature (T_m) of La-modified bismuth layer-structured ferroelectric ceramics has been reported earlier [33, 34] and was attributed to a decrease in the lattice distortion [35]. The variation of dissipation factor (tan δ) with temperature in La doped SBT ceramic is shown in Fig. 3b. It was observed that the dissipation factor decreases with increase in La content due to the decrease of structural deficiency because of incorporation of lanthanum. Again it can also be stated that the incorporation of La in Bi reduces the oxygen vacancy.

A modified empirical expression proposed by Uchino and Nomura [36] to describe the diffuse behaviour of ferroelectric phase transition and is given as

$$\frac{1}{\varepsilon} - \frac{1}{\varepsilon_m} = \frac{(T - T_m)^{\gamma}}{C} \quad (\text{at } T > T_m) \tag{2}$$

where the value of γ and C are assumed to be constant, lies between 1 and 2. The limiting values $\gamma = 1$ reduce the equation to modify Curie–Wiess law, valid for the case of normal ferroelectrics and $\gamma = 2$ valid for the relaxor

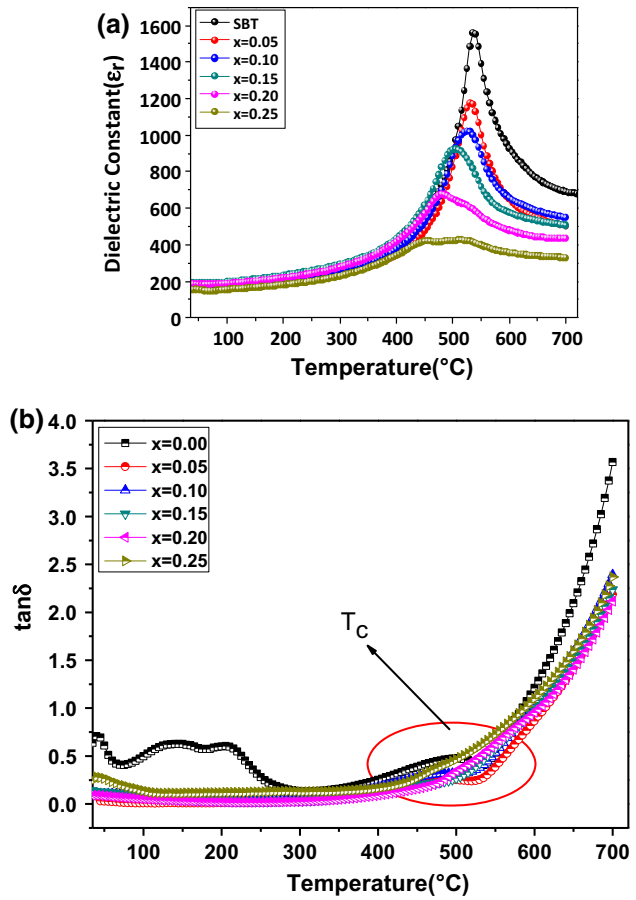

Fig. 3 **a** Temperature dependence of dielectric constant, **b** dielectric loss of La-doped SBT at frequency of 100 kHz

ferroelectrics, respectively. The logarithm of $(1/\varepsilon - 1/\varepsilon_m)$ was plotted against the logarithm of $(T - T_m)$ at 100 kHz shown in Fig. 4 and the slope gives the γ values. The γ values for all the compositions were presented in the Fig. 4. The diffuse transitions arises due to presence of two or three types of ions in A-sites of the perovskite layers. It was observed that diffusivity increases with increase in La content.

3.4 Ferroelectric properties

Figure 5 shows the room temperature (P-E) hysteresis loops of La doped SBT ceramics measured at 50 Hz frequency under a maximum electric field 60 kV/cm. The measured remnant polarization (P_r) and coercive field (E_c) values with varying La content (x) in SBT ceramics are listed in Table 1. It was observed that both the remnant polarization (P_r) and the coercive field increases with increasing La content up to $x = 0.15$, and thereafter decreases to lower values with further La content. The variation of P_r and E_c on La content (x) could be explained in terms of the changing oxygen vacancy concentration in the system. It is reported that oxygen vacancies are created due to bismuth loss, and under high electric fields the mobile oxygen vacancies can assemble at the lowest energy domain walls and thereby hinder polarization switching due to domain pinning [37]. At higher La content $x > 0.15$, the decrease in P_r was attributed to the relaxation in structural distortion as noted from X-ray and Raman spectroscopy study. It indicates that La^{3+} incorporation into the $(Bi_2O_2)^{2+}$ layer creates a cation disorder and a disturbance in the adjoining perovskite layers resulting in the relaxation of the structural distortion.

3.5 Impedance study

Figure 6 shows CIS Nyquist plot for La doped SBT composition at room temperature. The plots were depressed and off-centered which reflects a non-Debye type nature of these samples [31]. The existence of more than one semicircular arc again represents the presence of different relaxation processes; the low frequency window arc corresponds to the grain boundary relaxation mechanism, while the high frequency window arc to the grain relaxation. The experimental data were fitted with an equivalent circuit built up by cascading of the parallel combination of (1) a resistance (bulk resistance), capacitance (bulk capacitance) and a CPE, with another parallel combination of (2) a resistance (grain boundary resistance), capacitance

Table 1 Electrical properties of $SrBi_{4-x}La_xTi_4O_{15}$ ceramic at room temperature: ε_r dielectric constant, R_g grain resistance, R_{gb} grain boundary resistance, σ_{dc} dc conductivity, P_r remanent polarisation, E_c coercive field

Composition $SrBi_{4-x}La_xTi_4O_{15}$	ε_r (100 kHz)	R_g (Ω)	R_{gb} (Ω)	σ_{dc} (s/cm^2)	P_r (μC/cm^2)	E_c (kV/cm)
x = 0.0	162	17,304	1,076	7.26×10^{-4}	0.69	23.56
x = 0.05	177	18,069	880	9.82×10^{-4}	1.09	22.14
x = 0.10	181	15,623	758	1.0×10^{-3}	1.18	24.80
x = 0.15	194	9,936	609	1.41×10^{-3}	1.31	26.55
x = 0.20	185	22,740	2217	1.31×10^{-3}	0.96	22.88
x = 0.25	155	27,244	3083	8.84×10^{-4}	0.89	21.09

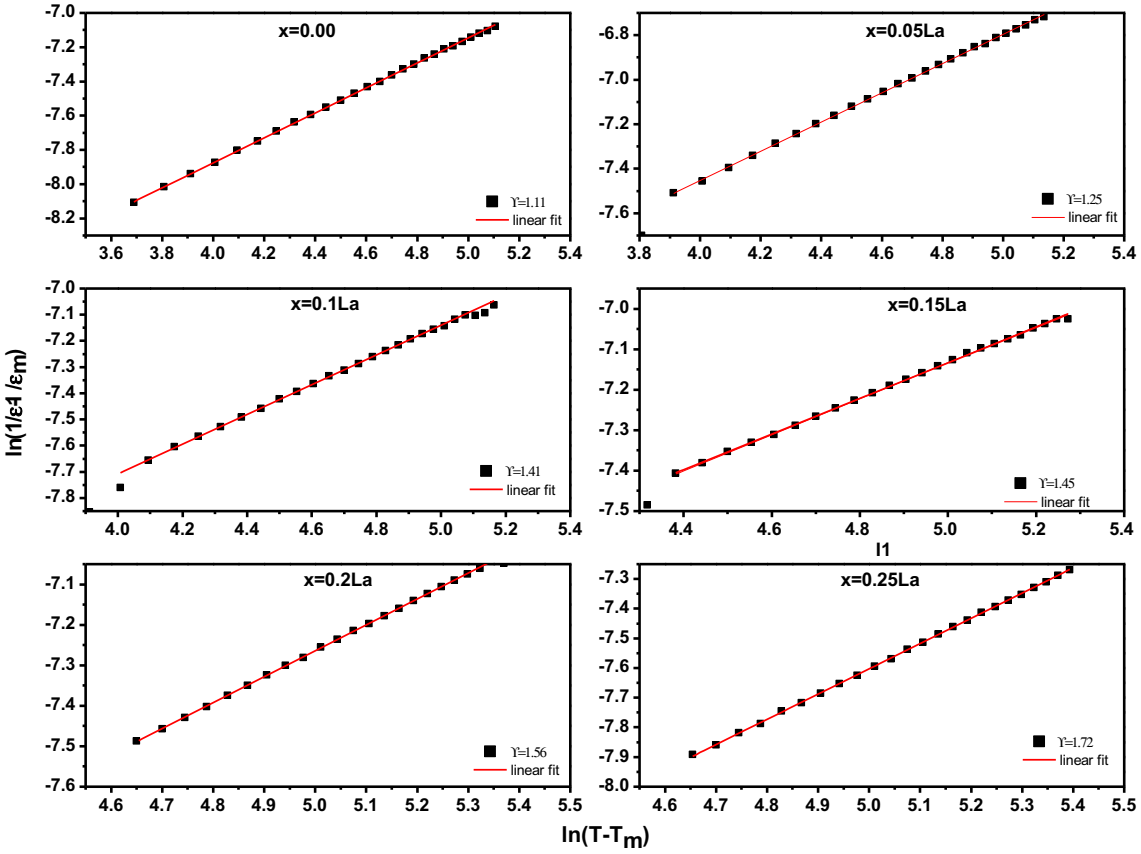

Fig. 4 Variation of $\ln(1/\varepsilon - 1/\varepsilon_m)$ as a function of $\ln(T - T_m)$

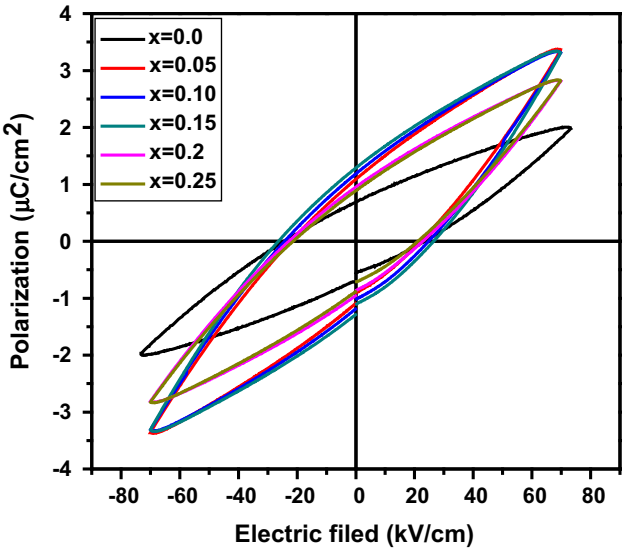

Fig. 5 P-E hysteresis loop of $SrBi_{4-x}La_xTi_4O_{15}$ ceramic

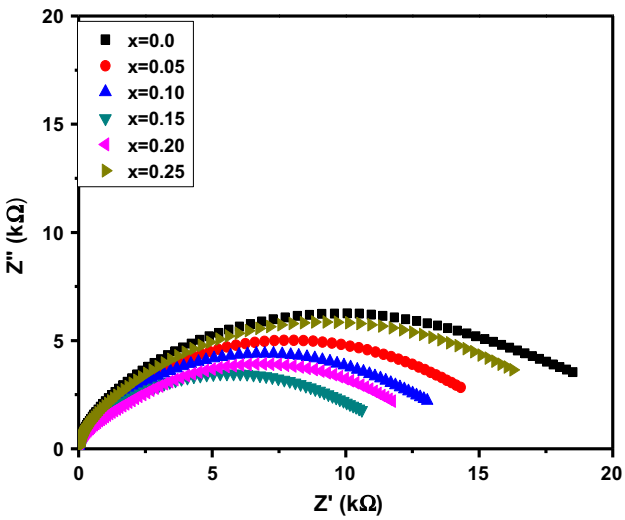

Fig. 6 The Nyquist plots for La-doped SBT ceramic at room temperature

(grain boundary capacitance) using commercially available Z Simp Win Version 3.2 software. The fitting values of the grain and grain boundary resistance were presented in Table 1. The grain (R_g) and grain boundary resistance (R_{gb}) decreases with increase in La content up to x = 0.15, then further increase with increase in La content.

3.6 Conductivity studies

Figure 7 shows the frequency dependence Ac conductivity (σ_{ac}) of La doped SBT composition at room temperature. The value of σ_{ac} increases with increase in the La-

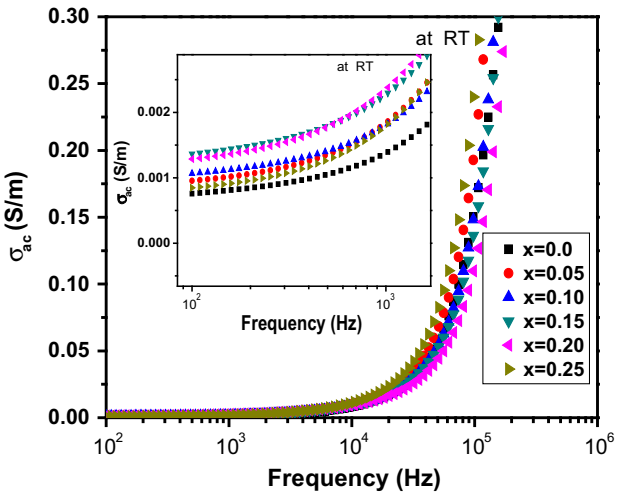

Fig. 7 Frequency dependence of the ac conductivity (σ_{ac}) at room temperature for $SrBi_{4-x}La_xTi_4O_{15}$ with composition x = 0.00, 0.05, 0.1, 0.15, 0.2, 0.25

concentration up to 0.15 and decreases with further La doping. It was also observed that the conductivity value increases with increasing frequency and a plateau was observed in the low frequency region. The extrapolation of the plateau regions where $\omega \rightarrow 0$ gives the DC conductivity (σ_{dc}) values of the material. After a certain frequency called the hopping frequency (ω_H) of charge carriers, σ_{ac} increases as power law fashion (Jonscher's) and the real part of conductivity for such a situation can be expressed as [29]

$$\sigma(\omega) = \sigma_{dc}\left[1 + \left(\frac{\omega}{\omega_H}\right)^n\right] \quad (3)$$

where n is the dimensionless frequency exponent. The hopping takes place by charge carriers through localization positions separated by energy barriers of varied heights [38]. The temperature dependent parameter, n represents the extent of many body interactions among charge carriers and defect states [39].

The DC conductivity can be calculated from the fitting of the above equation as shown in insert of Fig. 7. Apart from the structural distortion for $x > 0.15$, the pronounced site selectivity of La into the SBT ceramics leads to an asymmetric variation in the DC conductivity. It was observed that the DC conductivity increases up to $x = 0.15$ and then decreases with increase in La content. The variation of DC conductivity was related incorporation of La in the Perovskite layer and the $(Bi_2O_2)^{2+}$ layers. Similar kind of observation on the DC conductivity has been reported by Kumar and Verma [40] for La^{3+} substitution on BBT ceramics. It is suggested that the incorporation of La^{3+} ions into the $(Bi_2O_2)^{2+}$ layers appear to disturb the original functions of electrical insulation and space charge compensation of the $(Bi_2O_2)^{2+}$ layers [17].

4 Conclusion

Lanthanum doped SBT ceramic has been prepared by solid state reaction route. The variation in the structural, dielectric, ferroelectric and conductivity study were carried out with varying La content in the range (x = 0–0.25). The X-ray diffraction study has revealed that all the compositions are of single phase. The lattice parameter obtained from the X-ray study increases up to x = 0. 15, then decreases with further doping concentration. The shift in the Raman mode indicates preferred incorporation of La^{3+} ions at the A-site of the pseudo perovskite slabs for x = 0.15 whereas for $x > 0.15$, lanthanum has incorporated into the $(Bi_2O_2)^{2+}$ layers. It has been observed from the temperature dependent dielectric study that La content leads to a continuous lowering of the phase transition temperature and suppresses the maximum dielectric constant due to decrease in lattice distortion with increasing La content. The dielectric diffusivity increases with increase in La content. The room temperature P-E loop shows that the remnant polarization (P_r) and the coercive field (E_c) increase up to x = 0.15 and then decrease with further La doping. A similar kind of variation has been observed in the DC conductivity value. All the results clearly indicate that La has a different site occupancy in SBT ceramic and preferred incorporation at the A-site of the pseudo perovskite slabs up to x = 0. 15 whereas for $x > 0.15$, lanthanum has incorporated into the $(Bi_2O_2)^{2+}$ layers.

Acknowledgments One the authors (P. Nayak) acknowledge the financial support from the Department of science and Technology Grant No. SR/WOS-A/PM-1003/2014(G).

References

1. B. Aurivillius, Mixed bismuth oxides with layer lattices: I. The structure type of $CaNb_2Bi_2O_9$. Arkiv Kemi **1**(5), 463–480 (1949)
2. I.M. Reaney, D. Damjanovic, Crystal structure and domain-wall contributions to the piezoelectric properties of strontium bismuth titanate ceramics. J. Appl. Phys. **80**(7), 4223–4225 (1996)
3. N. Ramulu, G. Prasad, S. Suryanarayana, T. Bhima Sankaram, Studies on electrical properties of $SrBi_4Ti_{4-3x}Fe_{4x}O_{15}$. Bull. Mater. Sci. **23**, 431–437 (2000)
4. M. Raghavender, G.S. Kumar, G. Prasad, Electric properties of La modified strontium bismuth titanate ceramic. Indian J. Pure Appl. Phys. **44**, 46–51 (2006)
5. S. Hwee Ng, J.M. Xue, J. Wang, High temperature piezoelectric strontium bismuth titanate from mechanical activation of mixed oxides. J. Mater. Chem. Phys. **75**, 131–135 (2002)

6. M.W. Chu, M. Ganne, M.T. Caldes, L. Brohan, X-ray photoelectron spectroscopy and high resolution electron microscopy studies of Aurivillius compounds: $Bi_{4-x}La_xTi_3O_{12}$(x = 0, 0.5, 0.75, 1.0, 1.5, and 2.0). J. Appl. Phys. **91**, 3178–3187 (2002)
7. C.H. Park, D.J. Chadi, Microscopic study of oxygen-vacancy defects in ferroelectric perovskites. Phys. Rev. B **57**, R13961 (1998)
8. T. Mihara, H. Watanabe, C.A. Pas de Araujo, Unipolar and bipolar fatigue in antiferroelectric lead zirconate thin films and evidences for switching-induced charge injection inducing fatigue. J. Appl. Phys. **33**, 5186–5281 (1994)
9. D. Dimos, H.N. Al-Shareef, W.L. Warren, B.A. Tuttle, Photoinduced changes in the fatigue behavior of $SrBi_2Ta_2O_9$ and Pb (Zr, Ti) O_3 thin films. J. Appl. Phys. **80**, 1682–1687 (1996)
10. S. Maruno, T. Murao, T. Kuroiwa, N. Mikami, A. Tomikawa, T. Nagata, T. Yasue, T. Koshikawa, Effects of oxygen vacancy diffusion on leakage characteristics of Pt/$(Ba_{0.5}Sr_{0.5})TiO_3$/Pt capacitor. J. Appl. Phys. 2 **39**, L416 (2000)
11. W. Wang, S.P. Gu, X.Y. Mao, X.B. Chen, Effect of Nd modification on electrical properties of mixed-layer Aurivillius phase $Bi_4Ti_3O_{12}$–$SrBi_4Ti_4O_{15}$. J. Appl. Phys. **102**, 024102(1-9) (2007)
12. C.L. Diao, J.B. Xu, H.W. Zheng, L. Fang, Y.Z. Gu, W.F. Zhang, Dielectric and piezoelectric properties of cerium modified $BaBi_4Ti_4O_{15}$ ceramics. Ceram. Int. **39**, 6991–6995 (2013)
13. B.H. Park, B.S. Kang, S.D. Bu, T.W. Noh, J. Lee, W. Jo, A new ferroelectric material for FRAM applications: lanthanum-substituted bismuth titanate. Nat. (Lond.) **401**, 682–684 (1999)
14. A.Z. Simões, E.C. Aguiar, E. Longo, J.A. Varela, Retention characteristics of lanthanum-doped bismuth titanate films annealed at different furnaces. Mater. Chem. Phys. **115**, 434–438 (2009)
15. Y.Y. Yao, C.H. Song, P. Bao, D. Su, X.M. Lu, J.S. Zhu, Y.N. Wang, Doping effect on the dielectric property in bismuth titanate. J. Appl. Phys. **95**, 3126–3131 (2004)
16. A. Chakrabarti, J. Bera, Effect of La-substitution on the structure and dielectric properties of $BaBi_4Ti_4O_{15}$ ceramics. J. Alloys Compd. **505**, 668–674 (2010)
17. A. Khokhar, P.K. Goyal, O.P. Thakur, A.K. Shukla, K. Sreenivas, Influence of lanthanum distribution on dielectric and ferroelectric properties of $BaBi_{4-x}La_xTi_4O_{15}$ ceramics. Mater. Chem. Phys. **152**, 13–25 (2015)
18. J. Zhu, T. Xiao-Bing Chen, J. Cang Shen, Lanthanum distribution in $SrBi_{4-x}La_xTi_4O_{15}$. Mater. Lett. **59**, 1581–1584 (2005)
19. Y.P. Chen, Y.Y. Yao, Z.H. Bao, P. Bao, J.S. Zhu, Y.N. Wang, Study on ferroelectric and dielectric properties of La-doped $SrBi_4Ti_4O_{15}$ ceramics. Mater. Lett. **57**, 3623–3628 (2003)
20. S.K. Rout, E. Sinha, A. Hussain, J.S. Lee, C.W. Ahn, I.W. Kim, S.I. Woo, Phase transition in $ABi_4Ti_4O_{15}$ (A = Ca, Sr, Ba) Aurivillius oxides prepared through a soft chemical route. J. Appl. Phys. **105**, 024105 (2009)
21. J. Arreguin-Zavala, Cation distribution in the Bi_4–xRE xTi_3O_{12}(RE = La, Nd) solid solution and curie temperature dependence. Mater. Charact. **60**, 219–224 (2009)
22. A. Husur, Raman scattering study of A-and B-site substitutions in ferroelectric $Bi_4Ti_3O_{12}$. J. Korean Phys. Soc. **41**, 763–768 (2002)
23. W. Wang, S.P. Gu, X.Y. Mao, X.B. Chen, Structural and electrical characterization of chemical-solution-derived $Bi_5FeTi_3O_{15}$ thin films. J. Appl. Phys. **102**, 024102 (2007)
24. A. Khokhar, P.K. Goyal, K. Sreenivas, Site selectivity of Sm^{3+} ions in $BaBi_{4-x}Sm_xTi_4O_{15}$ ceramics and its influence on electrical properties. Mater. Lett. **160**, 408–411 (2015)
25. J. Zhu, X.B. Chen, Z.P. Zhang, J.C. Shen, Raman and X-ray photoelectron scattering study of lanthanum-doped strontium bismuth titanate. Acta Mater. **53**, 3155–3162 (2005)
26. S. Kojima, R. Imaizumi, S. Hamazaki, M. Takashige, Raman study of ferroelectric bismuth layer-oxides $ABi_4Ti_40_{15}$. J. Mol. Struct. **348**, 37–40 (1995)
27. J.B. Kennedya, Q. ZhouIandarb, Y. Kubotac, K. Katod, Cation disorder and phase transitions in the four-layer ferroelectric Aurivillius phases $ABi_4Ti_4O_{15}$ (A = Ca, Sr, Ba, Pb). J. Solid State Chem. **181**, 1377–1386 (2008)
28. H. Hao, H.X. Liu, M.H. Cao, X.M. Min, S.X. Ouyang, Study of A-site doping of $SrBi_4Ti_4O_{15}$ Bi-layered compounds using micro-Raman spectroscopy. Appl. Phys. A **85**, 69–73 (2006)
29. E.V. Raman, M.P.F. Graça, M.A. Valente, T.B. Sankaram, Improved ferroelectric and pyroelectric properties of Pb-doped $SrBi_4Ti_4O_{15}$ ceramics for high temperature applications. J. Alloys Compd. **583**, 198–205 (2014)
30. R.Z. Hou, X.M. Chen, Dielectric properties of La^{3+} substituted $BaBi_8Ti_7O_{27}$ ceramics. Mater. Res. Bull. **38**, 63–668 (2003)
31. Y. Shimakawa, Y. Kubo, Y. Tauchi, H. Asano, T. Kamiyama, F. Izumi, Z. Hiroi, Crystal and electronic structures of $Bi_{4-x}La_xTi_3O_{12}$ ferroelectric materials. Appl. Phys. Lett. **79**, 2791–2793 (2001)
32. Y. Kan, Lanthanum modified bismuth titanate prepared by a hydrolysis method. J. Mater. Chem. **14**, 3566–3570 (2004)
33. T. Takenaka, K. Sakata, Electrical properties of grain-oriented ferroelectric ceramics in some lanthanum modified layer structured oxides. Ferroelectrics **38**, 769–772 (1981)
34. V.K. Seth, W.A. Schulze, Grain-oriented fabrication of bismuth titanate ceramics and its electrical-properties. IEEE Trans. Ultrason. Ferroelectr. Freq. Control Soc. **36**, 41–49 (1989)
35. D.Y. Saurez, I.M. Reaney, W.E. Lee, Relation between tolerance factor and Tc in Aurivillius compounds. J. Mater. Res. **11**, 3139–3149 (2001)
36. K. Uchino, S. Nomura, Critical exponents of the dielectric constants in diffused-phase-transition crystals. Ferroelectr. Lett. **44**, 55 (1982)
37. Y. Noguchi, I. Miva, Y. Goshima, M. Miyayama, Defect control for large remanent polarization in bismuth titanate ferroelectrics—doping effect of higher-valent Cations. Jpn. J. Appl. Phys. **39**, L1259–L1262 (2000)
38. A. Khodorov, S.A.S. Rodrigues, M. Pereira, J.M. Gomes, Impedance spectroscopy study of a compositionally graded lead zirconate titanate structure. J. Appl. Phys. **102**, 114109 (2007)
39. P. Dhak, D. Dhak, M. Das, P. Pramanik, Dielectric and impedance spectroscopy study of $Ba_{0.8}Bi_{2.133}Nb_{1.6}Ta_{0.4}O_9$ ferroelectric ceramics, prepared by chemical route. J. Mater. Sci.: Mater. Electron. **22**, 1750–1760 (2011)
40. S. Kumar, K.B.R. Verma, Influence of lanthanum doping on the dielectric, ferroelectric and relaxor behaviour of barium bismuth titanate ceramics. J. Phys. D Appl. Phys. **42**, 075405 (2009)